

# Resurrecting Sneutrino ( $\tilde{\nu}_L$ ) Dark Matter in light of Neutrino Mass and LUX

Arindam Chatterjee\*

*Harish-Chandra Research Institute, Chhatnag Road, Jhusi, Allahabad, 211 019, India*

Narendra Sahu†

*Department of Physics, IIT Hyderabad,  
ODF campus, Yeddumailaram, 502205, AP, India*

## Abstract

In the minimal supersymmetric standard model (MSSM) the lightest superpartner of the left-handed neutrinos is ruled out of being a candidate of dark matter because of its large elastic cross-section with the nucleus mediated via Z-boson. We resurrect it by extending the MSSM with two triplets with opposite hypercharge. The addition of the triplets not only play a role in generating small Majorana masses for the left-handed active neutrinos but also make the lightest sneutrino a viable candidate for dark matter. We then discuss the relevant parameter space in details which can give rise to the right amount of (thermal) relic abundance as well as satisfy the current direct detection constraints from Xenon100 and LUX. We find that sneutrino dark matter with mass 370-550 GeV can give rise to right thermal relic abundance while co-annihilating with the bino-like neutralino.

---

\* arindam@hri.res.in

† nsahu@iith.ac.in

## I. INTRODUCTION

With the discovery of Higgs at LHC [1, 2], standard model (SM) of particle physics seems to be complete. However, the latter does not explain the non-zero neutrino mass, required to explain solar and atmospheric neutrino oscillation hypothesis, and the existence of non-baryonic dark matter (DM) required to explain the galaxy rotation curve, gravitational lensing and large scale structure of the Universe [3]. In fact, the relic abundance of DM:  $\Omega_{\text{DM}}h^2 \sim 0.12$ , is well measured by WMAP-9 [4] and Planck [5] satellites.

The above mentioned inadequacies of SM indicate that the present form of SM is not sufficient to explain the current energy budget of the Universe. It needs to be extended to include sub-eV masses of left-handed neutrinos and the observed DM abundance. If we assume that the neutrinos are of Majorana type, then their sub-eV masses can be accounted through seesaw mechanisms [6–12]. On the other hand, the relic abundance of DM can be accounted by adding an extra stable particle which is massive and electrically neutral.

A well motivated theory beyond the SM is the minimal supersymmetric standard model (MSSM) which may explain DM relic abundance and sub-eV masses of left-handed neutrinos. Within MSSM, if R-parity ( $R_p = (-1)^{(3B+L+2S)}$ ) is conserved, then it can easily accommodate a candidate for DM (see e.g. [13]). Because of conserved R-parity, the viable dark matter candidates are either the lightest neutralino ( $\tilde{\chi}_1^0$ ) or the lightest left-handed sneutrino ( $\tilde{\nu}_L$ ). It has been known since long that  $\tilde{\nu}_L$ , as an elastic DM candidate, is ruled out by direct search limits up to a very heavy mass, beyond which it can not produce the right (thermal) relic abundance [14]. This leaves  $\tilde{\chi}_1^0$  as the only viable candidate for DM within MSSM. On the other hand, if R-parity is broken in MSSM then the latter does not accommodate any candidate for DM, but can explain sub-eV Majorana masses of light neutrinos [15–18]. Thus a simultaneous explanation for sub-eV neutrino mass and DM does not exist within the framework of MSSM unless one adds new particles to the MSSM spectrum.

In this article we extend the MSSM with two  $SU(2)_L$  triplets [19] of opposite hypercharge, such as  $\hat{\Delta}_1(1, 3, 2)$  and  $\hat{\Delta}_2(1, 3, -2)$ , where the numbers in the parentheses are quantum numbers under the gauge group  $SU(3)_C \times SU(2)_L \times U(1)_Y$ . We also impose a global  $U(1)_{B-L}$  symmetry, where  $B$  and  $L$  are baryon and lepton number respectively. Consequently all the  $R$ -parity violating terms in the MSSM superpotential are forbidden. Note that in absence of  $U(1)_{B-L}$  or  $R$ -parity, the gauge symmetry of MSSM superpotential allows certain terms

which violate  $B$  and  $L$  numbers although they are strictly conserved within the SM. The  $U(1)_{B-L}$  global symmetry is allowed to be broken explicitly by the soft term  $\Delta_1 \tilde{L} \tilde{L}$  which also breaks the supersymmetry. However, the soft term has a residual symmetry,  $(-1)^L$  which is equivalent to a  $Z_2$  symmetry. As a result the neutral candidate of  $\tilde{L}$ , the sneutrino, as the lightest supersymmetric particle (LSP), is stable. After electroweak (EW) symmetry breaking the induced vacuum expectation value (vev) of  $\Delta_1$  generates a mass splitting between the real and imaginary parts of sneutrino. Assuming a mass splitting of few hundred KeV, the inelastic sneutrino (DM)-nucleon interaction mediated via  $Z$  can be avoided [20–22]. A proposed explanation of DAMA [23] requires a mass splitting of  $\mathcal{O}(100)$  KeV between the real and imaginary parts of  $\tilde{\nu}_L$ . Although such an explanation is disfavored by XENON 100 [24], a small window remains viable [25]. Moreover, small Majorana mass of neutrinos can be generated through one loop radiative process mediated by gaugino and sneutrino [26].

Since the triplets are heavy, their CP-violating out-of-equilibrium decay can generate an asymmetry between sneutrino and anti-sneutrino [19, 27] in the early Universe. However, this asymmetry can be washed out [27–29] after the EW-phase transition because of sneutrino-antisneutrino mixing. Therefore, we focus on the parameter space where sneutrino can have the right relic abundance through thermal freeze-out mechanism, and at the same time sub-eV neutrino masses can be generated. Co-annihilation of sneutrino plays an important role in the estimation of its thermal relic abundance. In particular, co-annihilation with the bino-like neutralino and with the lightest sbottom (or any other strongly interacting particle) can be important in obtaining the right thermal relic in case of relatively light and heavy sneutrinos respectively. Typically, co-annihilation with the bino-like neutralino allows sneutrino masses in the range 370-550 GeV to achieve the right thermal relic abundance.

The paper is arranged as follows. In section-II, we discuss the triplet extension of MSSM by focusing sneutrino as a viable candidate for DM and then express the relevant constraints from neutrino mass. Section-III is devoted to explain asymmetric sneutrino DM and its depletion through sneutrino anti-sneutrino oscillation. In section-IV, we discuss parameter space in which the sneutrino relic abundance can be generated through freeze-out mechanism. Section-V is devoted to discuss the constraints from direct detection of sneutrino DM. We conclude in section VI.

## II. SNEUTRINO ( $\tilde{\nu}_L$ ) DARK MATTER IN TRIPLET EXTENSION OF MSSM

We extend the MSSM superpotential by including two triplet super fields  $\hat{\Delta}_1(1, 3, 2)$  and  $\hat{\Delta}_2(1, 3, -2)$ , where the numbers in the parentheses are quantum numbers under the gauge group  $SU(3)_C \times SU(2)_L \times U(1)_Y$ . We then impose a global  $U(1)_{B-L}$  symmetry, which forbids all the  $R$ -parity violating terms in the MSSM superpotential. The relevant superpotential in presence of  $U(1)_{B-L}$  symmetry is given by:

$$\mathcal{W} \supset \mu \hat{H}_u \cdot \hat{H}_d + Y \hat{L} \cdot \hat{H}_d \hat{E}^c + M \hat{\Delta}_1 \cdot \hat{\Delta}_2 + f_1 \hat{\Delta}_1 \hat{H}_d \hat{H}_d + f_2 \hat{\Delta}_2 \hat{H}_u \hat{H}_u, \quad (1)$$

where we have suppressed the flavour indices. The corresponding Lagrangian then becomes:

$$\begin{aligned} -\mathcal{L} \supset & |\mu|^2 (|H_u|^2 + |H_d|^2) + M(|\Delta_1|^2 + |\Delta_2|^2) + |f_1|^2 |H_d|^4 + |f_2|^2 |H_u|^4 + 4|f_1|^2 |\Delta_1|^2 |H_d|^2 \\ & + 4|f_2|^2 |\Delta_2|^2 |H_u|^2 + \left[ 2f_1^* \mu \Delta_1^\dagger H_u H_d^\dagger + 2f_2^* \mu \Delta_2^\dagger H_d H_u^\dagger + f_1^* M \Delta_2 H_d^\dagger H_d^\dagger + f_2^* M \Delta_1 H_u^\dagger H_u^\dagger + \text{h.c.} \right] \\ & + |Y|^2 \left( \tilde{L}^\dagger \tilde{L} \right) \left( H_d^\dagger H_d + \tilde{E}^{c\dagger} \tilde{E}^c \right) + |Y|^2 \left( H_d^\dagger H_d \right) \left( \tilde{E}^{c\dagger} \tilde{E}^c \right) \\ & + \left( Y^* \mu H_u \tilde{L}^\dagger \tilde{E}^{c\dagger} + 2f_1 Y^* \Delta_1 H_d \tilde{L}^\dagger \tilde{E}^{c\dagger} + \text{h.c.} \right) \\ & + \mu (\tilde{H}_u \cdot \tilde{H}_d) + M(\tilde{\Delta}_1 \cdot \tilde{\Delta}_2) + f_1 \Delta_1 (\tilde{H}_d \cdot \tilde{H}_d) + f_2 \Delta_2 (\tilde{H}_u \cdot \tilde{H}_u) + 2f_1 \tilde{\Delta}_1 (H_d \cdot \tilde{H}_d) + 2f_2 \tilde{\Delta}_2 (H_u \cdot \tilde{H}_u) \\ & + Y(\tilde{L} \cdot \tilde{H}_d) E^c + Y \tilde{E}^c (L \cdot \tilde{H}_d) + Y(H_d \cdot L) E^c. \end{aligned} \quad (2)$$

The  $U(1)_{B-L}$  global symmetry is explicitly broken by the soft term  $\Delta_1 \tilde{L} \tilde{L}$  which also breaks the supersymmetry. However, the soft term has a residual symmetry,  $(-1)^L$  which is equivalent to a  $Z_2$  symmetry. As a result the neutral candidate of  $\tilde{L}$ , the sneutrino, can be a stable LSP. It will be shown later that it can be a good candidate for DM. In the effective theory, the relevant SUSY breaking terms in the Lagrangian are given by:

$$\mathcal{V}_{\text{soft}} \supset M_{\tilde{L}}^2 \tilde{L}^* \tilde{L} + MB \Delta_1 \Delta_2 + A_1 \Delta_1 H_d H_d + A_2 \Delta_2 H_u H_u + \mu_L \Delta_1 \tilde{L} \tilde{L} + \text{h.c.} \quad (3)$$

The co-efficient of  $\Delta_1 \tilde{L} \tilde{L}$  term, i.e.,  $\mu_L$  is required to be small as it breaks  $U(1)_{B-L}$ . The electroweak phase transition occurs when  $H_u$  and  $H_d$  acquire vacuum expectation values (vevs). They also induce small vevs for  $\Delta_1$  and  $\Delta_2$ . From Eqs. (2) and (3) we get the vevs of  $\Delta_1$  and  $\Delta_2$  to be

$$\begin{aligned} \langle \Delta_1 \rangle &\equiv u_1 = -(A_1 v_d^2 + f_2^* M v_u^2) / 2M^2 \\ \langle \Delta_2 \rangle &\equiv u_2 = -(A_2 v_u^2 + f_1^* M v_d^2) / 2M^2. \end{aligned} \quad (4)$$

As we will discuss, smallness of the mass of  $\nu$  requires  $u_1$  to be very small. In the subsequent analysis we further assume  $f_1$  and  $f_2$  to be less than  $\mathcal{O}(.1)$ . Thus the tree-level contribution to the MSSM Higgs potential from the triplets remain small.

### A. Inelastic Sneutrino Dark Matter and Constraints

Because of the induced vevs of scalar triplets the sneutrino and anti-sneutrino states mix with each other. The relevant mass term takes the following form :

$$\mathcal{L}_M = \frac{1}{2}(\tilde{\nu}_L \tilde{\nu}_L^*)^* \mathcal{M} (\tilde{\nu}_L \tilde{\nu}_L^*)^T, \quad (5)$$

where  $\mathcal{M}$  is given by,

$$\begin{pmatrix} M_{\tilde{L}}^2 + \frac{1}{2}M_Z^2 \cos 2\beta & \delta M_{\tilde{\nu}}^2 \\ \delta M_{\tilde{\nu}}^2 & M_{\tilde{L}}^2 + \frac{1}{2}M_Z^2 \cos 2\beta \end{pmatrix} \quad (6)$$

and  $\delta M_{\tilde{\nu}}^2 = \mu_L u_1$ . We have dropped the generation index in the above expressions. In terms of the CP-eigenstates  $\tilde{\nu}_L = (\tilde{\nu}_{rL} + i \tilde{\nu}_{iL})/\sqrt{2}$ . Consequently, the mass matrix in the basis:  $(\tilde{\nu}_{rL}, \tilde{\nu}_{iL})$  is given by,

$$\begin{pmatrix} M_{\tilde{L}}^2 + \frac{1}{2}M_Z^2 \cos 2\beta + \delta M_{\tilde{\nu}}^2 & 0 \\ 0 & M_{\tilde{L}}^2 + \frac{1}{2}M_Z^2 \cos 2\beta - \delta M_{\tilde{\nu}}^2 \end{pmatrix} \quad (7)$$

The eigenvalues are given by the diagonal entries and the mass eigenstates are given by

$$\tilde{\nu}_k \in \{\tilde{\nu}_{rL}, \tilde{\nu}_{iL}\} \quad \forall k \in \{1, 2\},$$

where the index  $k = 1$  denotes the lightest state. The mass splitting between the two eigenvalues  $\Delta M_{\tilde{\nu}} \equiv \sqrt{M_{\tilde{\nu}_2}^2 - M_{\tilde{\nu}_1}^2} = 2 \sqrt{|\delta M_{\tilde{\nu}}^2|} = 2\sqrt{|\mu_L u_1|}$ . Evading present direct detection bounds require  $\Delta M_{\tilde{\nu}} > \mathcal{O}(100)\text{KeV}$ . We will come back to this issue in details while discussing the direct detection constraints.

### B. Radiative Neutrino Mass and Constraints

At the tree level the Majorana masses of the active neutrinos are exactly zero as we have imposed an  $U(1)_{B-L}$  symmetry on the MSSM, which forbids not only the  $R$ -parity violating

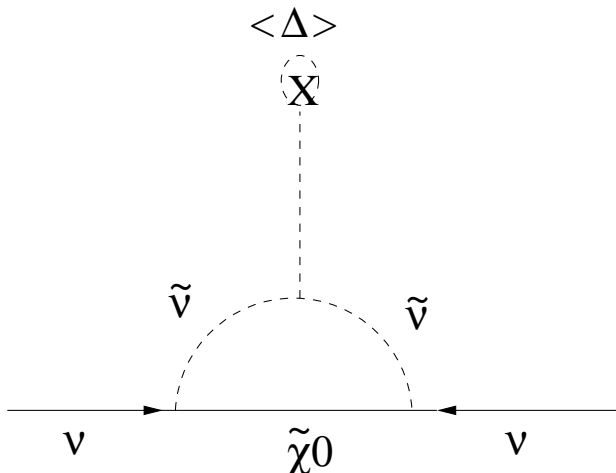


FIG. 1. Majorana mass of neutrinos generated through one loop radiative correction.

terms allowed by the MSSM superpotential, but also the  $\Delta_1 LL$  term. But the  $U(1)_{B-L}$  global symmetry is softly broken to a residual symmetry  $(-1)^L$  by the  $\mu_L \Delta_1 \tilde{L} \tilde{L}$ . As a result the neutrinos acquire masses through one loop radiative correction as shown in Fig. (IIB). The neutrino mass can be calculated from Fig. (IIB) as [19, 26]:

$$M_\nu = \frac{g^2}{32\pi^2 \cos \theta_w^2} \left[ \frac{\sin \theta_w^2 r_1}{r_1^2 - 1} \left( 1 - \frac{r_1^2}{r_1^2 - 1} \ln r_1^2 \right) + \frac{\cos \theta_w^2 r_2}{r_2^2 - 1} \left( 1 - \frac{r_2^2}{r_2^2 - 1} \ln r_2^2 \right) \right] \delta M_{\tilde{\nu}}, \quad (8)$$

where the ratios in Eq. (IIB) are defined by

$$r_1 = \frac{M_1}{M_{\tilde{\nu}}} \quad \text{and} \quad r_2 = \frac{M_2}{M_{\tilde{\nu}}}. \quad (9)$$

In the above Eq.  $M_1$  and  $M_2$  are soft-supersymmetry-breaking mass parameters for  $U(1)_Y$  and  $SU(2)_L$  gauginos, which, in the limit of no-mixing, give the masses of these states. The non-observation of DM at direct detection experiments require  $\Delta M_{\tilde{\nu}} > \mathcal{O}(100)\text{KeV}$ . On the other hand, the oscillation experiments require  $M_\nu < 1 \text{ eV}$ . Thus the ratio of neutrino mass to the mass splitting of sneutrino states can be given by:

$$R \equiv \frac{M_\nu}{\Delta M_{\tilde{\nu}}} < 10^{-5}. \quad (10)$$

We have shown the allowed values of  $r_1$  and  $r_2$  in Fig. (IIB) for all values of  $R < 10^{-5}$ . For simplicity, we have assumed a pure bino-like and a pure wino-like neutralino with mass  $|M_1|$  and  $M_2$  respectively. Note that, by defining mass eigenstates in the neutralino-chargino sector appropriately, it is possible to absorb the sign of either  $M_1$  or  $M_2$ . Thus, without loss

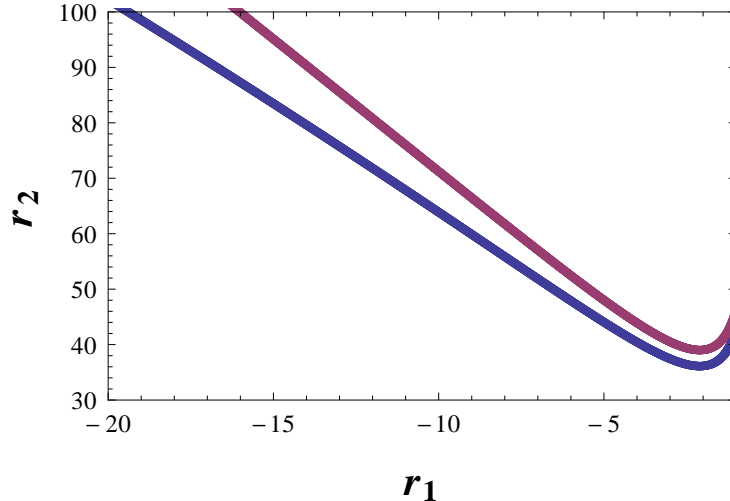


FIG. 2. Allowed values of  $r_1$  and  $r_2$  are shown for all value of  $0 < R < 10^{-5}$ . The blue and the pink line corresponds to  $R = 10^{-5}$  and  $R = 0$  respectively. We have assumed a pure bino-like and a pure wino-like state with masses  $|M_1|$  and  $M_2$  respectively.

of generality, we have assumed  $M_2 > 0$ . In order to allow for  $\Delta M_{\tilde{\nu}} > \mathcal{O}(100)\text{KeV}$   $M_1 < 0$  is required [19].

### III. ASYMMETRIC SNEUTRINO DARK MATTER (DM) AND DM - $\overline{\text{DM}}$ OSCILLATION

The scalar triplets  $\Delta_1$  and  $\Delta_2$  are required to be heavy ( $\mathcal{O}(10^{14}\text{GeV})$ ) in order to keep their vevs naturally small. Otherwise they will modify the  $\rho$  parameter of SM. In an expanding Universe  $\Delta_1$  and  $\Delta_2$  go out-of-equilibrium as the temperature falls below their mass scales. As a result the CP-violating out-of-equilibrium decay of the mass eigenstates, corresponding to  $\{\Delta_1, \Delta_2\}$ , to MSSM Higgses and sleptons can generate a net asymmetry between sleptons and anti-sleptons [19, 30, 31]. The asymmetry between the number densities of  $\tilde{\nu}_L$  and  $\tilde{\nu}_L^*$  can also be affected via the t-channel gaugino (and higgsino) mediated annihilation processes. These processes can annihilate a pair of  $\tilde{\nu}_L$  or  $\tilde{\nu}_L^*$  producing sleptons or anti-sleptons respectively. However, this interaction rate is, typically, weaker than the Z-mediated s-channel process, which annihilates the “symmetric” component, i.e. annihilates one  $\tilde{\nu}_L$  and

with one  $\tilde{\nu}_L^*$ <sup>1</sup>. This reduces the total number density of  $\tilde{\nu}_L$  and  $\tilde{\nu}_L^*$ , without affecting the relative excess of  $\tilde{\nu}_L$  compared to that of  $\tilde{\nu}_L^*$ . As a result one may expect a net asymmetric sneutrino dark matter.

### A. DM - $\overline{\text{DM}}$ Oscillation and Depletion of Sneutrino Asymmetry

After EW-phase transition the scalar triplets acquire small induced vevs. As a result the sneutrino ( $\tilde{\nu}_L$ ) and anti-sneutrino ( $\tilde{\nu}_L^*$ ) states mix with each other, thanks to the presence of  $\Delta L = 2$  terms in the Lagrangian. This creates a small mass splitting:  $\Delta M_{\tilde{\nu}}$  between the two mass eigen states:  $\tilde{\nu}_1$  and  $\tilde{\nu}_2$ . The splitting between the two mass eigenstates can drive an oscillation [27] as discussed below.

Let us write the sneutrino and anti-sneutrino states in terms of the mass eigenstates  $\tilde{\nu}_1$  and  $\tilde{\nu}_2$  as:

$$\begin{aligned} |\tilde{\nu}_L\rangle &= \frac{1}{\sqrt{2}} (\tilde{\nu}_1 + i\tilde{\nu}_2) \\ |\tilde{\nu}_L^*\rangle &= \frac{1}{\sqrt{2}} (\tilde{\nu}_1 - i\tilde{\nu}_2) \end{aligned} \quad (11)$$

The state  $|\tilde{\nu}_L\rangle$  at any space-time point  $(x, t)$  is given by

$$|\phi(x, t)\rangle = \frac{1}{\sqrt{2}} \left[ e^{-i(E_{\tilde{\nu}_1}t - k_{\tilde{\nu}_1}x)} |\tilde{\nu}_1\rangle + ie^{+i(E_{\tilde{\nu}_2}t - k_{\tilde{\nu}_2}x)} |\tilde{\nu}_2\rangle \right], \quad (12)$$

where  $E_{\tilde{\nu}_1} = \sqrt{k_{\tilde{\nu}_1}^2 + M_{\tilde{\nu}_1}^2}$  and  $E_{\tilde{\nu}_2} = \sqrt{k_{\tilde{\nu}_2}^2 + M_{\tilde{\nu}_2}^2}$  are the energy of  $\tilde{\nu}_1$  and  $\tilde{\nu}_2$  states respectively. The probability of  $|\tilde{\nu}_L\rangle$  oscillating into  $|\tilde{\nu}_L^*\rangle$  is then given by

$$P_{|\tilde{\nu}_L\rangle \rightarrow |\tilde{\nu}_L^*\rangle} = |\langle \tilde{\nu}_L^* | \phi(x, t) \rangle|^2. \quad (13)$$

Using Eqs. (11) and (12) the probability of oscillation takes the form:

$$P_{|\tilde{\nu}_L\rangle \rightarrow |\tilde{\nu}_L^*\rangle} = \frac{1}{4} \left[ 2 - e^{-i[(E_{\tilde{\nu}_1} - E_{\tilde{\nu}_2})t - (k_{\tilde{\nu}_2} - k_{\tilde{\nu}_1})x]} - e^{+i[(E_{\tilde{\nu}_1} - E_{\tilde{\nu}_2})t - (k_{\tilde{\nu}_2} - k_{\tilde{\nu}_1})x]} \right]. \quad (14)$$

Above the EW phase transition there is no mass splitting between the two mass eigenstates:  $\tilde{\nu}_1$  and  $\tilde{\nu}_2$ . Therefore we must have  $M_{\tilde{\nu}_1} = M_{\tilde{\nu}_2}$ ,  $E_{\tilde{\nu}_1} = E_{\tilde{\nu}_2}$  and  $k_{\tilde{\nu}_1} = k_{\tilde{\nu}_2}$ . As a result from Eq. 14 the probability of oscillation is:

$$P_{|\tilde{\nu}_L\rangle \rightarrow |\tilde{\nu}_L^*\rangle} = 0. \quad (15)$$

---

<sup>1</sup> There are t-channel neutralino mediated processes which also annihilate the ‘‘symmetric’’ component.

However, their contribution is only secondary to the Z-mediated s-channel process.



Below the EW phase transition the vev of  $\Delta$  generates a mass splitting between the two mass eigenstates  $\tilde{\nu}_1$  and  $\tilde{\nu}_2$ . Hence from Eq. 14, the probability of oscillation can be given by:

$$P_{|\tilde{\nu}_L\rangle\rightarrow|\tilde{\nu}_L^*\rangle} \simeq \frac{1}{2} \left[ 1 - \cos \left( \frac{\Delta M_{\tilde{\nu}}^2 (t - t_{\text{EW}})}{2E_{\tilde{\nu}}} \right) \right], \quad (16)$$

where we have assumed  $E_{\tilde{\nu}_1} \sim E_{\tilde{\nu}_2} \sim E_{\tilde{\nu}}$ , which is a good approximation for a small mass splitting. In the following we will consider a mass splitting of  $\mathcal{O}(100\text{keV})$ . We also count the time of evolution from the time of EW phase transition, so that at  $t = t_{\text{EW}}$ ,  $P_{|\tilde{\nu}_L\rangle\rightarrow|\tilde{\nu}_L^*\rangle} = 0$ . Below EW phase transition the time of oscillation from  $\tilde{\nu}_L$  to  $\tilde{\nu}_L^*$  can be estimated to be:

$$t - t_{\text{EW}} = \frac{2E_{\tilde{\nu}}\pi}{\Delta M_{\tilde{\nu}}^2}. \quad (17)$$

In the relativistic limit the energy of the DM particle  $E_{\tilde{\nu}} \sim T$ , where  $T$  is the temperature of the thermal bath. Hence the oscillation time can be given as:

$$t - t_{\text{EW}} \sim 4 \times 10^{-14} \text{Sec} \left( \frac{T}{100\text{GeV}} \right) \left( \frac{10^4 \text{keV}^2}{\Delta M_{\tilde{\nu}}^2} \right). \quad (18)$$

On the other hand, in the non-relativistic limit the energy of the DM particle  $E_{\tilde{\nu}} \sim M_{\tilde{\nu}}$ . Thus for  $M_{\tilde{\nu}} \sim 100 \text{ GeV}$ , the time of oscillation is again similar to relativistic case. This implies that if the mass eigenstates  $\tilde{\nu}_1$  and  $\tilde{\nu}_2$  remain in the thermal equilibrium, then oscillations between these two states can wash out the generated asymmetry through triplet decay [27–29]. As a result we may not get any asymmetric sneutrino relic abundance.

In order to prevent the catastrophic washout,  $\tilde{\nu}$  needs to decouple from the thermal soup before the creation of mass splitting at EW symmetry breaking (EWSB). Assuming EWSB occurs at around 100 GeV, and considering that the freeze-out temperature ( $T_f$ ) is approximately given by  $\frac{M_{\tilde{\nu}_1}}{20}$ , this requires the mass of sneutrino DM to be  $\mathcal{O}(2 \text{ TeV})$ . However, in a scenario where, for example, if the reheat temperature after inflation is less than  $\mathcal{O}(100 \text{ GeV})$  then this requirement may not hold good.

If the mass of the DM,  $M_{\tilde{\nu}_1}$ , is less than about  $\mathcal{O}(2 \text{ TeV})$ , then the initial asymmetry would not affect the relic density significantly. Therefore, we do not take into account the effect of any initial asymmetry into the present discussion. Thus, the relic density calculation resembles the case of a  $\tilde{\nu}$  Dark Matter [14, 32]. <sup>2</sup>

<sup>2</sup> The tiny mass splitting of  $\mathcal{O}(100) \text{ KeV}$  between the states  $\tilde{\nu}_1$  and  $\tilde{\nu}_2$  can be ignored when these are in the thermal soup, since the freeze-out temperature  $\mathcal{O}(10) \text{ GeV}$  is much higher compared to the splitting. The life-time of  $\tilde{\nu}_2$ , decaying to  $\tilde{\nu}_1 \bar{\nu} \nu$ , has been estimated to be  $10^4 - 10^9$  seconds for a mass splitting of 100 KeV-1 MeV [19]. After freezing-out  $\tilde{\nu}_2$  eventually decays to  $\tilde{\nu}_1$ . Also, due to very small decay width of  $\tilde{\nu}_2$ , we ignore the effect of its width in estimating the oscillation probability.

#### IV. SNEUTRINO DARK MATTER AND THERMAL RELIC ABUNDANCE

Assuming sufficiently high reheat temperature, and that all SUSY particles thermalized in the early universe, we will focus on the thermal production of  $\tilde{\nu}_1$  Dark Matter in this section.

However, a few alterations/variations have been incorporated in the present discussion. Instead of expanding  $\langle\sigma v_{\text{rel}}\rangle$  into the leading  $s$  and  $p$  wave contributions (ignoring the higher partial waves, and assuming no threshold or pole in the vicinity), we have used `micrOMEGAS` [33, 34] for an accurate estimate of  $\langle\sigma v_{\text{rel}}\rangle$ , and therefore, of the relic density. `SuSpect` [35] has been used as the spectrum generator. Assuming standard cosmology, we have used the recent estimates for the right (thermal) relic density from the CMBR measurements by `PLANCK` [5] and `WMAP` (9 year data)[4]. In addition, we have taken into account the recent bounds on the sparticle spectrum, especially on the CP-even Higgs mass (125 GeV) from the LHC [1, 2].

The computation of thermal relic abundance of the DM relies on various (co-)annihilation processes. This is discussed in some detail in Appendix B. In fact, in the absence of co-annihilations,  $\Omega_{DM}h^2 \propto \frac{1}{\langle\sigma_{ann}v\rangle}$  [36]. In the presence of co-annihilations, the DM and the co-annihilating sparticle remain in relative thermal equilibrium for a longer period of time through  $DM SM \rightarrow DM' SM'$ , where  $DM'$  denotes the co-annihilating sparticle;  $SM$  and  $SM'$  denote two Standard Model particles, which are assumed to be in thermal equilibrium and therefore abundant. Of course, eventually  $DM'$  decouples and decays to DM. Thus, co-annihilation affects the thermal relic abundance of DM. The effect can be captured by [37] substituting,

$$\sigma_{ann} \rightarrow \sigma_{eff} = \sum_{i,j} \frac{g_i g_j}{g_{eff}^2} (1 + \Delta_i)^{3/2} (1 + \Delta_j)^{3/2} e^{-x(\Delta_i + \Delta_j)} \sigma_{ij}, \quad (19)$$

where,  $\{i, j\}$  runs over the list of co-annihilating sparticles,  $g_i$  denotes the number of degrees of freedom of the  $i$ -th sparticle,  $\Delta_i = \frac{m_i}{m_{DM}} - 1$ ,  $x = \frac{m_{DM}}{T}$  and  $\sigma_{ij}$  denotes the co-annihilation cross-section of  $i$  and  $j$ -th sparticles into SM particles. Also,

$$g_{eff} = \sum_i g_i (1 + \Delta_i)^{3/2} e^{-x\Delta_i}.$$

Thus, co-annihilations are only relevant for sufficiently small  $\Delta_i$ .

Note that, there is always a (left) slepton of the same flavor as the  $\tilde{\nu}_L$ , with a small mass difference, thanks to the soft-breaking masses preserving the  $SU(2)_L$  invariance [14].

So, apart from “co-annihilation” with  $\tilde{\nu}_2$ , co-annihilation with the  $SU(2)_L$  doublet partner will always be relevant. The dominant contributions to the relic abundance comes from the s-channel  $Z$  mediated processes which annihilates a pair of  $\tilde{\nu}_1, \tilde{\nu}_2$  to SM particles. The possible final states, for the mass-range of our interest, are  $\{f\bar{f}, W^\pm W^\mp, Zh\}$ . Note that, due to our choice of a rather heavy  $m_A$ , the heavy neutral and charged Higgses can not occur in the final states. Also, the four point vertices contribute to  $\{ZZ, W^\pm W^\mp, hh\}$  in final states. The processes with a pair of light fermion and anti-fermion in the final state are p-wave suppressed. So their contributions remain insignificant. Co-annihilation with the  $SU(2)_L$  partner, via  $W^\pm$  exchange also contributes. As we will elaborate, we further include co-annihilation with various other sparticles, which can have significant impact on the relic density, opening up more parameter space where  $\tilde{\nu}_1$  produces the right thermal relic.

For the numerical analysis we have made the following assumptions.

- For the first two generations, the squark mass parameters are assumed to be 2 TeV. For the 3rd generation, left (right) handed squarks are assumed to have soft masses around 3 (1.5) TeV. This choice alleviates LHC constraints from direct SUSY searches and helps to achieve the lightest Higgs boson mass of  $\sim 125$  GeV. The gluino mass parameter ( $M_G$ ) is fixed at 1.5 TeV.
- The soft-SUSY breaking slepton masses are assumed to be flavor-diagonal.
- Trilinear soft susy breaking terms  $A_t = -3.7$  TeV and  $A_b = -3.7$  TeV;  $A_\tau = 0$  TeV;  $\tan\beta = 10$  and the CP-odd Higgs mass  $m_A = 1$  TeV have been assumed.
- We refrain from exact calculation of neutrino masses and mixing angles.  $M_1 < 0$  is assumed keeping  $M_2 > 0$ , in order to cancel the large radiative contribution to the neutrino masses.  $\mu = -1000$  GeV is assumed, except in the context of co-annihilation with higgsino-like neutralinos.
- Finally we use 173.1 GeV for the top quark pole mass.

In the following we consider three scenarios in the framework of pMSSM:

- A)  $\tilde{\nu}_1$  DM, with no other co-annihilating sparticles except the above mentioned ones;
- B)  $\tilde{\nu}_1$  DM co-annihilating also with a bino-like neutralino ( $\tilde{\chi}_1^0$ );

parameter	A	B		C	D
		(1)	(2)		
$M_1$	-1000	-388.8	-312.4	-1200	-1100
$\mu$	-1000	-1000	-1000	-677	-1500
$m_{\tilde{L}_3}$	580	385	310	690	1000
$m_{\tilde{R}}$	1000	1000	1000	1000	2000
$m_{\tilde{\nu}_\tau}$	571.6	379.9	303.6	687.1	998
$m_{\tilde{\nu}_e}$	998	496	303.6	998	2000
$m_{\tilde{\nu}_\mu}$	998	496	303.6	998	2000
$m_{\tilde{\chi}_1^0}$	962.6	380.1	303.9	687.2	1090
$\Omega_h^2$	0.1	0.1	0.12	0.1	0.12

TABLE I. Columns (A), (B1), (C) and (D) demonstrate benchmark points for scenarios (A), (B), (C) and (D) respectively. Column (B2) depicts a scenario where all three generations of  $\tilde{\nu}$  are degenerate, and are co-annihilating with a bino-like  $\tilde{\chi}_1^0$ . All the masses are in GeV.

- C)  $\tilde{\nu}_1$  DM co-annihilating also with a higgsino-like  $\tilde{\chi}_1^0$  (and possibly  $\tilde{\chi}_1^\pm$ ).
- D)  $\tilde{\nu}_1$  DM co-annihilating also with the lightest  $\tilde{b}$  ( $\tilde{b}_1$ ).

As shown in Fig. II B, since small neutrino masses require a -ve  $M_1$  and rather large  $M_2$ ; therefore, we refrain from discussing co-annihilation with a wino-like  $\tilde{\chi}_1^0$  (and possibly  $\tilde{\chi}_1^\pm$ ). The benchmark points are shown in table I. The contribution of various (co-)annihilation channels, in each case, can be found in Appendix A.

In benchmark (A), we consider a scenario where  $\tilde{\nu}_1$  belongs to the third generation, and has no additional co-annihilation channels except the above mentioned ones. The dominant contributions come from  $\tilde{\nu}_1, \tilde{\nu}_2$  (or  $\tilde{\nu}, \tilde{\nu}^*$ ) annihilating to  $Z Z$  (27%) and  $W^\pm W^\mp$  (24%). While both receive contributions from 4-point vertices involving  $\tilde{\nu}\tilde{\nu}^*, ZZ/W^\pm W^\mp$ , the  $Z$  mediated  $s$ -channel process also contributes to the latter. There are  $t$ -channel processes mediated by  $\tilde{\nu}$  and  $\tilde{\tau}$ , which also contribute to  $ZZ$  and  $W^\pm W^\mp$  respectively. Among co-annihilation channels with (the dominantly left handed)  $\tilde{\tau}_1, W^- \gamma$  and  $W^- Z$  contribute about 9% each. These processes originate from four-point vertices, as well as from  $W$ -boson exchange in the  $s$ -channel, while a  $t$ -channel contribution mediated by  $\tilde{\tau}$  contributes

sub-dominantly. The effective annihilation cross-section, as in eq. (19) receives further contributions from  $\tilde{\tau}_1\tilde{\tau}_1^*$  annihilation into  $W^\pm W^\mp$ , again from the four-point vertices, and also via  $s$ -channel  $Z$  exchange and  $t$ -channel  $\tilde{\tau}$  exchange diagrams respectively. Note that all these dominant processes have  $SU(2)_L$  gauge couplings appearing in the vertices.

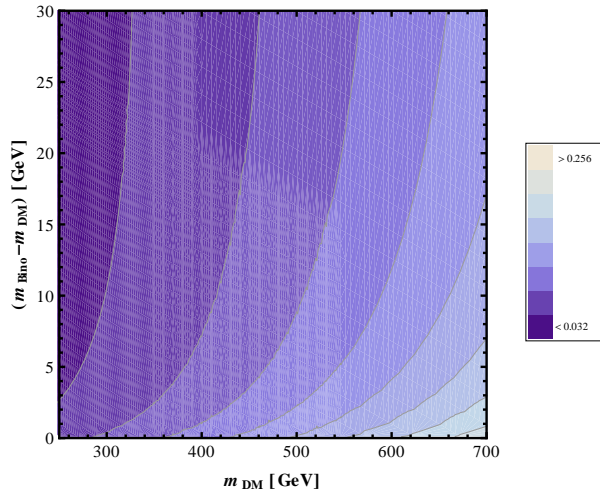


FIG. 3. This figure shows the variation of the thermal relic density of  $\tilde{\nu}_1$  DM, as a function of its mass and the mass difference with a bino-like  $\tilde{\chi}_1^0$ .

In benchmark (B1), we consider further co-annihilation with a bino-like  $\tilde{\chi}_1^0$ . The mass splitting between the  $\tilde{\chi}_1^0$  and  $\tilde{\nu}_1$  (and  $\tilde{\nu}_2$ ) is about 200 MeV. A small mass splitting is kept to enhance the effect of the co-annihilation. The (co-)annihilation processes involving a bino-like  $\tilde{\chi}_1^0$  involves  $U(1)_Y$  gauge coupling, which is less than  $SU(2)_L$  gauge coupling,  $\sigma_{eff}$  effectively becomes smaller. This contributes in a little early freeze-out of  $\tilde{\nu}_1$  increasing the relic abundance. Thus, we get the right thermal relic for a lower mass of  $\tilde{\nu}_1$ , which is about 380 GeV. The dominant co-annihilation channel, in this case, is  $\tilde{\chi}_1^0\tilde{\nu} \rightarrow W^+\tau$  via  $s$ -channel  $\nu$  mediation and via  $t$ -channel  $\tilde{\tau}$  mediation. It contributes about 8%. Another process  $\tilde{\chi}_1^0\tilde{\nu} \rightarrow Z\nu_\tau$ , via  $s$ -channel  $\nu$  mediation and via  $t$ -channel  $\tilde{\nu}_\tau$  mediation contributes about 5%. Note that, since the contribution from the charge conjugate final states are also included, the final states for the former are twice (i.e.  $W^+\tau$  and  $W^-\bar{\tau}$ ) that of the latter, leading to a larger contribution. In benchmark (B2) we consider a similar scenario, with three degenerate  $\tilde{\nu}$ . This can be achieved if the soft-mass for  $SU(2)_L$  doublet sleptons are independent of generation. We focussed on obtaining the right thermal relic density for the

lightest possible  $\tilde{\nu}$  Dark Matter. We obtain the right thermal relic with sneutrino of mass 303.6 GeV. We have ignored flavor mixing in the sneutrino (and slepton) sector. So the dominant (co-)annihilation processes remain the same for three generations. Figure 3 shows the variation of relic density as we vary the bino-mass parameter  $M_1$ . In this figure, we do not assume any degeneracy for all three generations of  $\tilde{\nu}$ . It demonstrates that for suitable mass difference of  $\tilde{\nu}_1$  and the bino-like  $\tilde{\chi}_1^0$ , one can have the right relic density in the mass range of 370-550 GeV.

In benchmark (C), we consider co-annihilation with the higgsino-like neutralinos and chargino. This can be achieved considering the  $\mu$  parameter to be close to the soft-breaking mass for  $\tilde{\nu}_\tau$ . Unlike the bino, higgsinos come from  $SU(2)_L$  doublets, and possesses relatively stronger interactions. Since in the limit of large  $M_2$ , and  $|M_1| \gg \mu$  three states  $\tilde{\chi}_1^0$ ,  $\tilde{\chi}_2^0$  and  $\tilde{\chi}_1^\pm$  are higgsino-like. Therefore, their impact on  $\sigma_{eff}$  is quite large. The leading contribution comes from  $\tilde{\chi}_1^+ \tilde{\chi}_1^0 \rightarrow \{u\bar{d}, s\bar{c}\}$ , each contributing 8%. These occur dominantly via  $s$ -channel  $W^\pm$  exchange processes. Since  $SU(2)_L$  gauge coupling appear in both vertices and because of the colour factor the total contribution is large. Similar  $W^\pm$  mediated  $s$ -channel processes producing leptons contribute about 3% each. Since  $\tilde{\chi}_2^0$  is also higgsino-like,  $\tilde{\chi}_1^+ \tilde{\chi}_2^0$  also annihilates to similar final states. However, because of the larger mass-splitting between  $\tilde{\nu}_1$  and  $\tilde{\chi}_2^0$ , its contribution to  $\sigma_{eff}$  is little less.

Finally, in benchmark (D) we consider co-annihilation with the lightest  $\tilde{b}$ , which we have assumed to be dominantly  $SU(2)_L$ -singlet-type. The mass of  $\tilde{b}_1$  is assumed to be 1008.4 GeV. The dominant contribution to the effective thermal averaged cross-section comes from  $\tilde{b}_1 \tilde{b}_1^* \rightarrow g g$ ;  $s$ -channel gluon mediation, as well as  $t$ (and  $u$ )-Chennai  $\tilde{b}_1$  exchange processes lead to this final state. This receives large enhancement due to the colour factor. The gluino mediated  $t$ (and  $u$ ) channel process  $\tilde{b}_1 \tilde{b}_1 \rightarrow bb$  also contributes significantly. Together, these channels contribute about 80%, as described in Table V. There are also small contributions from  $\tilde{\nu} \tilde{\nu}^*$ ,  $ZZ/W^\pm W^\mp$ .

In fig. IV, the green line denote the thermal relic density with no additional co-annihilations present. Further, this figure demonstrates that co-annihilations with bino-like  $\tilde{\chi}_1^0$  (blue line) leads to an increment in the relic density. We chose  $|M_1| - M_{\tilde{L}} = 5$  GeV.

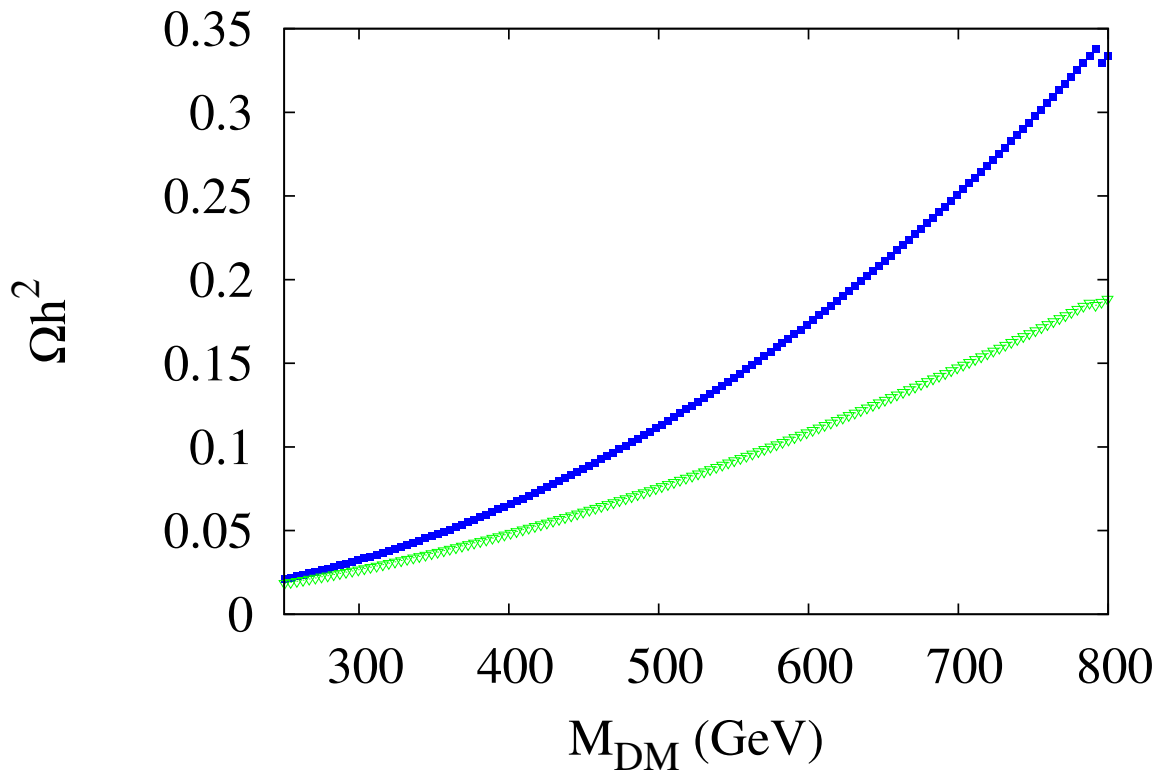


FIG. 4. Relic abundance for  $\tilde{\nu}_1$  Dark Matter has been shown. The green dots represent a scenario when no additional co-annihilation is present; while the blue dots represent co-annihilation scenario with a bino-like  $\tilde{\chi}_0^1$ . The bino mass parameter ( $|M_1|$ ) have been assumed to be 5 GeV above  $M_{\text{DM}}$  in the latter scenario.

## V. SNEUTRINO DARK MATTER AND DIRECT DETECTION CONSTRAINTS

In this section we review the viability of left-handed sneutrino dark matter by taking into account the latest direct detection constraints from Xenon-100 [38] and LUX [39]. As mentioned before, the *dominant process* through which the sneutrino DM interacts with the nucleon is the  $t$ -channel  $Z$ -boson mediated process, i.e.  $\tilde{\nu}q \rightarrow Z \rightarrow \tilde{\nu}q$ . Assuming sneutrino DM scattering off nucleon elastically, we have shown the DM-nucleon cross-section as a function of sneutrino mass in the left panel of fig. 5. From there we see that the cross-section is quite large and hence excludes sneutrino DM if the latter scatters off nucleon elastically through  $t$ -channel  $Z$ -boson mediated process. However, in the current set up,

the triplet extension of MSSM, the sneutrino DM scatters off nucleon inelastically through the  $Z$ -boson mediated process as we have discussed in section-II. The inelastic scattering:  $\tilde{\nu}_1 q \rightarrow \tilde{\nu}_2 q$  occurs depending on the mass splitting between the two nearly degenerate states:  $\tilde{\nu}_1$  and  $\tilde{\nu}_2$ . The minimum required velocity of the sneutrino dark matter (say  $\tilde{\nu}_1$ ) with respect to the earth frame that will lead to a recoil inside the detector is given by:

$$v_{min} = c \sqrt{\frac{1}{2M_N E_R}} \left( \frac{M_N E_R}{\mu_n} + \Delta M_{\tilde{\nu}} \right). \quad (20)$$

If we assume that  $\Delta M_{\tilde{\nu}}$  to be a few hundred keV, then to deposit energy inside the detector we need  $v_{min} > v_{esc} = 650 \text{ km/s}$ . In other words, if the mass splitting between  $\tilde{\nu}_1$  and  $\tilde{\nu}_2$  is larger than a few hundred KeV, then sneutrino can not scatter off nucleon inelastically through t-channel  $Z$ -boson mediated process.

The next dominant processes through which the sneutrino scatters off nucleon are the Higgs exchange processes occurring via the D-term. These processes receive contributions from both the CP-even Higgs bosons. The corresponding spin-independent cross-section, with a nucleus (N) of mass number  $A$  and atomic number  $Z$  can be expressed as,

$$\sigma_0 = \frac{\mu^2}{4\pi m_{\tilde{\nu}_1}^2} (A f_p + (A - Z) f_n)^2, \quad (21)$$

where  $\mu = \frac{m_{\tilde{\nu}_1} m_N}{m_{\tilde{\nu}_1} + m_N}$ ;  $m_N$  denotes the mass of the nucleus. Further,  $f_p$  and  $f_n$  denotes effective couplings of the CP-even Higgses with proton and neutron respectively. These are given by,

$$f^N = m_N \left( \sum_q^{u,d,s} f_q^N \frac{\lambda_q}{m_q} + \frac{2}{27} \sum_Q^{c,b,t} f_G \frac{\lambda_Q}{m_Q} \right); N \in \{p, n\}. \quad (22)$$

In the above expression  $\lambda_q$  denotes the effective coupling of  $\tilde{\nu}_1$  with the quark  $q$  (i.e.  $\mathcal{L}_{eff} \supset \lambda_q \tilde{\nu}_1^2 \bar{q}q$ ) in the limit of small momentum transfer, as is relevant for direct detection. Thus,  $\lambda_q$  is suppressed by  $m_{h/H}^2$  and is proportional to the  $SU(2)_L$  gauge coupling ( $g_2$ ), the appropriate Higgs VEV and the Yukawa coupling for quark  $q$  ( $y_q$ ).  $f_q^N$  denotes the contribution of quark  $q$  to the mass  $m_N$  of nucleon  $N$ . Note that, for large  $\tan \beta$ , the Yukawa couplings of the heavy Higgs (H) with down-type quarks can be large, and thus contributions from the heavy Higgs mediated channels can be significant. While the light quarks contribute to the nucleon masses directly, the heavy quark contributions to  $f^N$  appears through the loop-induced interactions with gluons. These are given by,

$$f_q^N = \frac{1}{m_N} \langle N | m_q \bar{q}q | N \rangle, \quad f_G = 1 - \sum_q^{u,d,s} f_q^N. \quad (23)$$



Using `micrOMEGAs-3.2`, with  $\tan\beta = 10$  and  $m_H \simeq 500$  GeV, we estimate that the direct detection cross-sections fall below the present LUX bounds for the mass range of our interest. For example, a 300 GeV  $\tilde{\nu}_1$  ( $\tau$ -type) has a direct detection cross-section of  $2 \times 10^{-45} \text{cm}^2$  which is about half the limit from LUX. With  $\tan\beta = 15$  and  $m_H \simeq 2000$  GeV, the interaction cross-section with neutrons have been plotted in fig. 5. The cross-section with protons is also similar. Note that, the strange quark content of the nucleon has significant uncertainties,

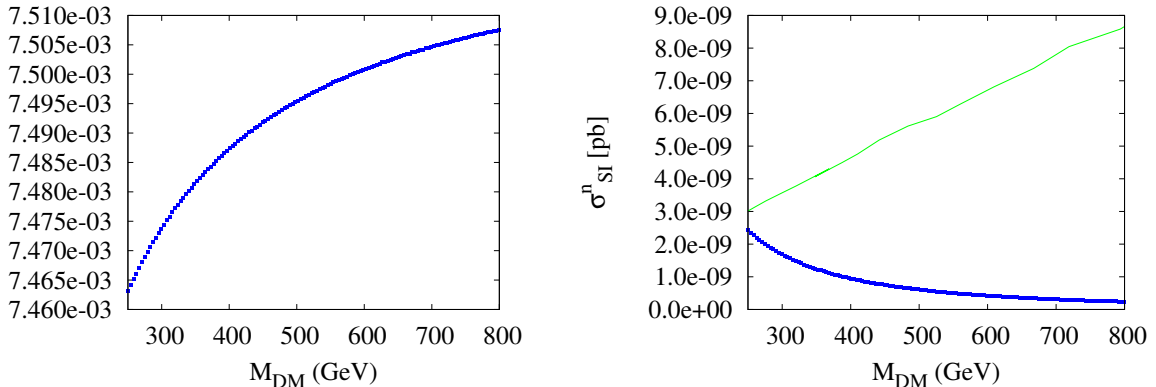


FIG. 5. The left panel of this figure shows the cross-section of the  $\tilde{\nu}_\tau$  DM with neutron as a function of its mass. Note that this includes the  $Z$  boson exchange processes. In the right panel, the blue line shows the Higgs exchange elastic cross-section of  $\tilde{\nu}_1$  DM with nucleon, while the green line corresponds to the experimental bound from LUX.

leading to an uncertainty in  $f_s^N$ . In the Higgs mediated processes, the  $s$ -quark content plays an important role, due to its large Yukawa coupling. We have used the default values in `micrOMEGAs-3.2` to estimate the cross-section. Note that by varying  $f_s^N$  it is possible to reduce the direct detection cross-section even further.

## VI. CONCLUSION

We discussed the viability of left-handed sneutrino ( $\tilde{\nu}_L$ ) as a candidate for DM in the triplet extension of the minimal supersymmetric standard model (MSSM). We extended the MSSM with two triplets of opposite hypercharges and imposed a global  $U(1)_{B-L}$  symmetry. The  $B - L$  symmetry is then allowed to break explicitly by a  $\Delta L = 2$  term ( $\Delta_1 \tilde{L} \tilde{L}$ ) which has a residual  $Z_2$  symmetry. As a result the lightest left-handed sneutrino became stable

and a viable candidate for DM. It is worth mentioning that within MSSM, sneutrino is ruled out as a candidate for (elastic) DM because of its large direct detection cross-section with the nucleus mediated via  $Z$ -boson. However, in the triplet extension of MSSM, this problem has been eradicated by creating a mass splitting between the real and imaginary parts of the sneutrino DM. By choosing the mass splitting to be a few hundred KeV, the  $Z$ -mediated process  $\tilde{\nu}_1 q \rightarrow Z \rightarrow \tilde{\nu}_1 q$  is forbidden. We then discussed the elastic scattering of sneutrino DM with the nucleon via the Higgs exchange processes. In fact, we found that for a 300 GeV sneutrino DM mass, the DM-nucleon cross-section is approximately  $2 \times 10^{-45} \text{cm}^2$  which is about half the limit from LUX.

Assuming that sneutrino is in thermal equilibrium in the early Universe, we estimated its relic density. We showed that, in a large part of the parameter space, co-annihilation of sneutrino plays an important role in the relic abundance estimation. In particular, assuming that mass splitting with the bino-like neutralino is small, we showed that the allowed mass of DM is in the range of 370-550 GeV. Note that for such range of sneutrino mass, the LUX bound is completely evaded.

Since the lepton number is broken explicitly by two units, the Majorana masses of light neutrinos could be generated at loop level. Further, since the additional triplets are very heavy, the model resembles MSSM in the energy accessible to the LHC. In summary, the salient features of this scenario include a very heavy wino and the possibility of having a  $\tilde{\nu}_L$ -type LSP which is a suitable candidate for DM. In future we will explore its collider phenomenology in detail.

## ACKNOWLEDGEMENT

We would like to thank the organizers of the Workshop on High Energy Physics and Phenomenology (WHEPP13), held at Puri, Odisha, India during 12-21 December 2013 where the foundation of this work was laid. We would also like to thank Debottam Das for useful discussions during the initial stage. NS is partially supported by the Department of Science and Technology Grant SR/FTP/PS-209/2011.

## APPENDIX A

In this appendix, we sketch the thermal relic density calculation[36, 40]. We assume that, to begin with, all the sparticles and the SM particles were in thermal equilibrium, forming a thermal soup. However, as the expansion rate of the universe exceeds the interaction rate (of the interactions which kept the species in thermal equilibrium) of a particle species, they decouple from the thermal soup. Due to the conserved R-parity, the total number of sparticles (in the early universe) is reduced only by their annihilation into the SM particles. Therefore the relevant number density to consider, to begin with, is the number density of all the sparticles (say  $n$ ), since the remaining ones (not annihilating into the SM particles) will decay to the  $\tilde{\nu}_1$  eventually contributing to the number density of  $\tilde{\nu}_1$ . The Boltzmann equation, governing the the evolution of the number density  $n$ , (in the FRW background, see e.g. [36]) can be written as,

$$\frac{dn}{dt} + 3Hn = -\langle\sigma v\rangle(n^2 - n_{eq}^2), \quad (24)$$

where  $n_{eq}^2$  denotes the equilibrium abundance. In this equation the second term in the left hand side arises due the expansion of the universe, the Hubble parameter being denoted by  $H$ . To scale out the effect due to the expansion of the universe, one often uses  $\frac{n\tilde{\nu}_1}{s}$ , where  $s$  denotes the entropy density to rewrite the above equation as,

$$\frac{dY}{dT} = \sqrt{\frac{\pi g_*(T)}{45}} M_p \langle\sigma v\rangle (Y(T)^2 - Y_{eq}(T)^2), \quad (25)$$

where  $T$  stands for the temperature,  $Y = \frac{n\tilde{\nu}_1}{s}$ ,  $g_*$  is an effective number relativistic degrees of freedom and  $M_p$  is the Planck mass. In order to express the time derivative in terms of the temperature derivative, conservation of the comoving entropy has been used, which gives  $\frac{dT}{dt} = -H$ , where  $H$ , as mentioned already, is the Hubble parameter. Note that, therefore, late <sup>3</sup> production of entropy (although not possible in the present scenario) will alter this discussion, see e.g. [13, 36]. Further,  $\langle\sigma v\rangle$  represents the relativistic thermally averaged (effective) annihilation cross-section of superparticles (into the SM particles) and

---

<sup>3</sup> By late we mean after the freeze-out of  $\tilde{\nu}_1$ , i.e. after the rate of the reaction pair producing  $\tilde{\nu}_1$  falls behind the Hubble expansion rate (given by the Hubble parameter  $H$ ).

is expressed as,<sup>4</sup>

$$\langle \sigma v \rangle = \frac{\sum_{i,j} g_i g_j \int_{(m_i+m_j)^2} ds \sqrt{s} K_1(\sqrt{s}/T) p_{ij}^2 \sigma_{ij}(s)}{2T \left( \sum_i g_i m_i^2 K_2(m_i/T) \right)^2}. \quad (26)$$

In eq.(26), the sum over  $i, j$  spans over all the sparticles,  $m_i$  denote the mass of sparticle (labeled by)  $i$ ,  $\sigma_{ij}$  denotes the annihilation cross-section of the sparticles  $i$  and  $j$  into the SM particles,  $p_{ij}$  and  $\sqrt{s}$ <sup>5</sup> denote the momentum and the total energy of the “incoming” sparticles in their center-of-mass frame.  $K_1$  and  $K_2$  denote modified Bessel functions of type one and two respectively. Eq.(25) can not be solved exactly by analytical means, a discussion on approximate solution can be found, e.g., in [36]. However, we have used the publicly available code `micrOMEGAs` for the relic density calculation which solves eq.(26) numerically without any approximation. For thermal averaging, we consider only sparticles ( $i, j$ ) such that the Boltzmann suppression factor  $e^{-A}$ , where  $A = \left( \frac{m_i + m_j - 2m_{\tilde{\nu}_1}}{T} \right)$  less than  $10^{-6}$ , which is (more than) sufficient for our purpose.

Solving eq.(26) by integrating over  $T_F$  to  $T_0$ ,  $T_0$  being the present CMBR temperature, gives the present value of  $Y$ , which we denote by  $Y_0$ . The present relic density, then, as a fraction of the critical density (which corresponds to a “flat” universe) can be expressed as,

$$\Omega_{0\tilde{\nu}_1} h^2 = \frac{\rho_{\tilde{\nu}_1}}{\rho_{crit}} h^2 = \frac{m_{\tilde{\nu}_1} s_0 Y_0}{\rho_{crit}} h^2 = 2.742 \times m_{\tilde{\nu}_1} Y_0 / \text{GeV}. \quad (27)$$

where  $\rho_{crit} = \frac{3H_0^2}{8\pi G}$ , with  $H_0$  and  $G$  denoting the (present) Hubble’s parameter and the gravitational constant respectively and  $s_0$  denotes the present entropy density.

## APPENDIX B

In this Appendix, we mention the (co-)annihilation channels which contribute more than 1% to the relic density, in case of the benchmark points shown in Table I. We obtain these estimates from `micrOMEGAs`. Because of the tiny mass splitting between  $\tilde{\nu}_1$  and  $\tilde{\nu}_2$ , we simply use  $\tilde{\nu}$  and  $\tilde{\nu}^*$  instead in the following tables. Note that we have ignored any flavor oscillation in the sneutrino sector. While introducing the flavor oscillations will not affect

---

<sup>4</sup> Since the freeze-out of the species under consideration occurs at a temperature well below its mass, typically  $T_F \sim m/20$ , Maxwell-Boltzmann statistics have been used in eq.(26).

<sup>5</sup> Note that we have also used “s” for the entropy density.

the relic density in a significant manner; it will affect the relative contributions from flavor dependent final states. We mention all relevant channels contributing more than 1% to the relic density.

Initial states	Final states	Contribution to $\Omega_{DM}^{-1}$ (in %)
$\tilde{\nu}_\tau \tilde{\nu}_\tau^*$	$W^+ W^-$	27
$\tilde{\nu}_\tau \tilde{\nu}_\tau^*$	$Z Z$	24
$\tilde{\tau}_1 \tilde{\nu}_\tau^*$	$\gamma W^-$	10
$\tilde{\tau}_1 \tilde{\tau}_1^*$	$W^+ W^-$	9
$\tilde{\tau}_1 \tilde{\nu}_\tau^*$	$Z W^-$	9
$\tilde{\tau}_1 \tilde{\nu}_\tau^*$	$W^- h$	6
$\tilde{\tau}_1 \tilde{\tau}_1^*$	$\{\gamma \gamma, h h\}$	3
$\tilde{\tau}_1 \tilde{\tau}_1^*$	$\gamma Z$	2
$\tilde{\tau}_1 \tilde{\nu}_\tau^*$	$\bar{t} b$	1

TABLE II. Contribution from various annihilation and co-annihilation channels to the relic density of  $\tilde{\nu}_1$  Dark Matter, for benchmark (A) of table I.

Initial states	Final states	Contribution to $\Omega_{DM}^{-1}$ (in %)
$\tilde{\nu}_\tau \tilde{\nu}_\tau^*$	$W^+ W^-$	28
$\tilde{\nu}_\tau \tilde{\nu}_\tau^*$	$Z Z$	24
$\tilde{\chi}_1^0 \tilde{\nu}_\tau$	$W^+ \tau$	8
$\tilde{\tau}_1 \tilde{\nu}_\tau^*$	$\gamma W^-$	6
$\tilde{\tau}_1 \tilde{\nu}_\tau^*$	$Z W^-$	5
$\tilde{\chi}_1^0 \tilde{\nu}_\tau$	$Z \nu_\tau$	5
$\tilde{\tau}_1 \tilde{\tau}_1^*$	$W^+ W^-$	4
$\tilde{\nu}_\tau \tilde{\nu}_\tau^*$	$h h$	3
$\tilde{\tau}_1 \tilde{\nu}_\tau^*$	$W^- h$	2
$\tilde{\nu}_\tau \tilde{\nu}_\tau$	$\nu_\tau \nu_\tau$	1
$\tilde{\tau}_1 \tilde{\tau}_1^*$	$\{\gamma \gamma, \gamma Z\}$	1
$\tilde{\nu}_\tau \tilde{\nu}_\tau^*$	$t \bar{t}$	1
$\tilde{\tau}_1 \tilde{\nu}_\tau^*$	$\bar{t} b$	1

TABLE III. Contribution from various annihilation and co-annihilation channels to the relic density of  $\tilde{\nu}_1$  Dark Matter, for benchmark (B1) of table I.

Initial states	Final states	Contribution to $\Omega_{DM}^{-1}$ (in %)
$\tilde{\nu}_i \tilde{\nu}_i^*$	$W^+ W^-$	30
$\tilde{\nu}_i \tilde{\nu}_i^*$	$Z Z$	27
$\tilde{\chi}_1^0 \tilde{\nu}_i$	$W^+ l_i$	9
$\tilde{\chi}_1^0 \tilde{\nu}_i$	$Z \nu_i$	6
$\tilde{\nu}_i \tilde{\nu}_i^*$	$h h$	3
$\tilde{l}_i \tilde{\nu}_i^*$	$\gamma W^-$	3
$\tilde{l}_i \tilde{\nu}_i^*$	$Z W^-$	3

TABLE IV. Contribution from various annihilation and co-annihilation channels to the relic density of  $\tilde{\nu}_1$  Dark Matter, for benchmark (B2) of table I. The subscript  $i \in \{1, 2, 3\}$  denotes generation.

Initial states	Final states	Contribution to $\Omega_{DM}^{-1}$ (in %)
$\tilde{b}_1 \tilde{b}_1^*$	$g g$	58
$\tilde{b}_1 \tilde{b}_1$	$b b$	19
$\tilde{\nu}_\tau \tilde{\nu}_\tau^*$	$W^+ W^-$	3
$\tilde{\nu}_\tau \tilde{\nu}_\tau^*$	$Z Z$	3
$\tilde{b}_1 \tilde{b}_1^*$	$\gamma g$	2
$\tilde{\tau}_1 \tilde{\nu}_\tau^*$	$\gamma W^-$	2
$\tilde{\tau}_1 \tilde{\tau}_1^*$	$W^+ W^-$	1
$\tilde{\tau}_1 \tilde{\nu}_\tau^*$	$Z W^-$	1

TABLE V. Contribution from various annihilation and co-annihilation channels to the relic density of  $\tilde{\nu}_1$  Dark Matter, for benchmark (D) of table I. The subscript  $i \in \{1, 2, 3\}$  denotes generation.

Initial states	Final states	Contribution to $\Omega_{DM}^{-1}$ (in %)
$\tilde{\chi}_1^+ \tilde{\chi}_1^0$	$\{u \bar{d}, \bar{s} c\}$	8
$\tilde{\chi}_1^+ \tilde{\chi}_2^0$	$\{u \bar{d}, \bar{s} c\}$	5
$\tilde{\nu}_\tau \tilde{\nu}_\tau^*$	$\{W^+ W^-, Z Z\}$	3
$\tilde{\chi}_1^0 \tilde{\chi}_1^0$	$W^+ W^-$	3
$\tilde{\chi}_1^+ \tilde{\chi}_1^0$	$\{\nu_e \bar{e}, \nu_\mu \bar{m}, \nu_\tau \bar{l}\}$	3
$\tilde{\chi}_1^0 \tilde{\chi}_2^0$	$\{d \bar{d}, s \bar{s}, b \bar{b}, u \bar{u}, c \bar{c}\}$	2
$\tilde{\chi}_1^0 \tilde{\chi}_1^0$	$Z Z$	2
$\tilde{\chi}_1^+ \tilde{\chi}_1^-$	$\{W^+ W^-, u \bar{u}, c \bar{c}, t \bar{t}\}$	2
$\tilde{\chi}_1^+ \tilde{\chi}_1^0$	$t \bar{b}$	2
$\tilde{\chi}_1^+ \tilde{\chi}_2^0$	$\{\nu_e \bar{e}, \nu_\mu \bar{m}, \nu_\tau \bar{l}\}$	2
$\tilde{\chi}_1^+ \tilde{\chi}_2^0$	$t \bar{b}$	1
$\tilde{\chi}_1^+ \tilde{\chi}_1^0$	$\gamma W^+$	1
$\tilde{\chi}_1^+ \tilde{\chi}_1^-$	$\{d \bar{d}, s \bar{s}\}$	1
$\tilde{\tau}_1 \tilde{\nu}_\tau^*$	$\gamma W^-$	1
$\tilde{\chi}_1^0 \tilde{\chi}_2^0$	$\{\nu_e \bar{\nu}_e, \nu_\mu \bar{\nu}_\mu, \nu_\tau \bar{\nu}_\tau\}$	1
$\tilde{\tau}_1 \tilde{\tau}_1^*$	$W^+ W^-$	1

TABLE VI. Contribution from various annihilation and co-annihilation channels to the relic density of  $\tilde{\nu}_1$  Dark Matter, for benchmark (C) of table I.



- 
- [1] G. Aad *et al.* (ATLAS Collaboration), Phys.Lett. **B716**, 1 (2012), arXiv:1207.7214 [hep-ex].
- [2] S. Chatrchyan *et al.* (CMS Collaboration), Phys.Lett. **B716**, 30 (2012), arXiv:1207.7235 [hep-ex].
- [3] G. Bertone, D. Hooper, and J. Silk, Phys.Rept. **405**, 279 (2005), arXiv:hep-ph/0404175 [hep-ph].
- [4] G. Hinshaw *et al.* (WMAP), Astrophys.J.Suppl. **208**, 19 (2013), arXiv:1212.5226 [astro-ph.CO].
- [5] P. Ade *et al.* (Planck Collaboration), (2013), arXiv:1303.5076 [astro-ph.CO].
- [6] P. Minkowski, Phys.Lett. **B67**, 421 (1977).
- [7] T. Yanagida, Conf.Proc. **C7902131**, 95 (1979).
- [8] R. N. Mohapatra and G. Senjanovic, Phys.Rev.Lett. **44**, 912 (1980).
- [9] M. Magg and C. Wetterich, Phys.Lett. **B94**, 61 (1980).
- [10] G. Lazarides, Q. Shafi, and C. Wetterich, Nucl.Phys. **B181**, 287 (1981).
- [11] R. N. Mohapatra and G. Senjanovic, Phys.Rev. **D23**, 165 (1981).
- [12] E. Ma and U. Sarkar, Phys.Rev.Lett. **80**, 5716 (1998), arXiv:hep-ph/9802445 [hep-ph].
- [13] M. Drees, R. Godbole, and P. Roy, *Theory and phenomenology of sparticles: An account of four-dimensional N=1 supersymmetry in high energy physics*, hackensack, USA: World Scientific (2004) 555 p.
- [14] T. Falk, K. A. Olive, and M. Srednicki, Phys.Lett. **B339**, 248 (1994), arXiv:hep-ph/9409270 [hep-ph].
- [15] F. Borzumati, Y. Grossman, E. Nardi, and Y. Nir, Phys.Lett. **B384**, 123 (1996), arXiv:hep-ph/9606251 [hep-ph].
- [16] M. A. Diaz, J. C. Romao, and J. Valle, Nucl.Phys. **B524**, 23 (1998), arXiv:hep-ph/9706315 [hep-ph].
- [17] R. Barbier, C. Berat, M. Besancon, M. Chemtob, A. Deandrea, *et al.*, Phys.Rept. **420**, 1 (2005), arXiv:hep-ph/0406039 [hep-ph].
- [18] G. Bhattacharyya, Nucl.Phys.Proc.Suppl. **52A**, 83 (1997), arXiv:hep-ph/9608415 [hep-ph].
- [19] E. Ma and U. Sarkar, Phys.Rev. **D85**, 075015 (2012), arXiv:1111.5350 [hep-ph].

- [20] L. J. Hall, T. Moroi, and H. Murayama, Phys.Lett. **B424**, 305 (1998), arXiv:hep-ph/9712515 [hep-ph].
- [21] D. Tucker-Smith and N. Weiner, Phys.Rev. **D64**, 043502 (2001), arXiv:hep-ph/0101138 [hep-ph].
- [22] D. Tucker-Smith and N. Weiner, Phys.Rev. **D72**, 063509 (2005), arXiv:hep-ph/0402065 [hep-ph].
- [23] R. Bernabei, P. Belli, F. Cappella, V. Caracciolo, S. Castellano, *et al.*, Eur.Phys.J. **C73**, 2648 (2013), arXiv:1308.5109 [astro-ph.GA].
- [24] E. Aprile *et al.* (XENON100 Collaboration), Phys.Rev. **D84**, 061101 (2011), arXiv:1104.3121 [astro-ph.CO].
- [25] C. Arina, R. N. Mohapatra, and N. Sahu, Phys.Lett. **B720**, 130 (2013), arXiv:1211.0435 [hep-ph].
- [26] Y. Grossman and H. E. Haber, Phys.Rev.Lett. **78**, 3438 (1997), arXiv:hep-ph/9702421 [hep-ph].
- [27] C. Arina and N. Sahu, Nucl.Phys. **B854**, 666 (2012), arXiv:1108.3967 [hep-ph].
- [28] M. R. Buckley and S. Profumo, Phys.Rev.Lett. **108**, 011301 (2012), arXiv:1109.2164 [hep-ph].
- [29] M. Cirelli, P. Panci, G. Servant, and G. Zaharijas, JCAP **1203**, 015 (2012), arXiv:1110.3809 [hep-ph].
- [30] T. Hambye, E. Ma, and U. Sarkar, Nucl.Phys. **B602**, 23 (2001), arXiv:hep-ph/0011192 [hep-ph].
- [31] E. J. Chun and S. Scopel, Phys.Rev. **D75**, 023508 (2007), arXiv:hep-ph/0609259 [hep-ph].
- [32] J. S. Hagelin, G. L. Kane, and S. Raby, Nucl.Phys. **B241**, 638 (1984).
- [33] G. Belanger, F. Boudjema, A. Pukhov, and A. Semenov, Comput.Phys.Commun. **174**, 577 (2006), arXiv:hep-ph/0405253 [hep-ph].
- [34] G. Belanger, F. Boudjema, A. Pukhov, and A. Semenov, Comput.Phys.Commun. **185**, 960 (2014), arXiv:1305.0237 [hep-ph].
- [35] A. Djouadi, J.-L. Kneur, and G. Moultaka, Comput.Phys.Commun. **176**, 426 (2007), arXiv:hep-ph/0211331 [hep-ph].
- [36] E. Kolb and M. Turner, *The Early Universe* (Westview Press, 1994).
- [37] Griest, Kim and Seckel, David, Phys. Rev. D **43**, 3191 (1991).

- [38] E. Aprile *et al.* (XENON100 Collaboration), Phys.Rev.Lett. **109**, 181301 (2012), arXiv:1207.5988 [astro-ph.CO].
- [39] D. Akerib *et al.* (LUX Collaboration), (2013), arXiv:1310.8214 [astro-ph.CO].
- [40] J. Edsjo and P. Gondolo, Phys.Rev. **D56**, 1879 (1997), arXiv:hep-ph/9704361 [hep-ph].